ChemComm

Accepted Manuscript

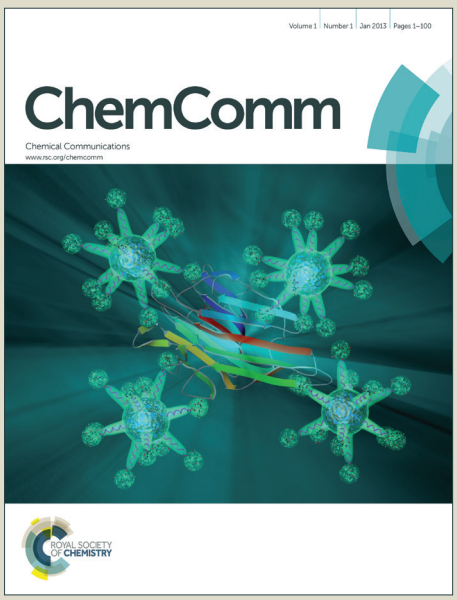

ROYAL SOCIETY OF CHEMISTRY

www.rsc.org/chemcomm

Journal Name

RSCPublishing

COMMUNICATION

Cite this: DOI: 10.1039/x0xx00000x

Received ooth January 2012,
Accepted ooth January 2012

www.rsc.org/

Self-assembling triazolophanes: From croissants through donuts to spherical vesicles

V. Haridas,*[a] Appa Rao Sapala[a] and Jerry P Jasinski *[b]

Macrocyclic compounds M1-M3 with different ring sizes containing amide and triazole units were synthesized. These triazolophanes displayed a variety of self-assembled structures such as hemi-toroids, toroids, and vesicles in a concentration dependent manner. Detailed ultramicroscopic and crystallographic investigations delineated a hierarchical mechanism of self-assembly.

The physico-chemical basis of morphogenesis continues to intrigue the scientists for over half a century.[1] The formations and transformations of biomolecular assemblies are intricately linked with the molecular structure. The link between functional biomolecular assemblies and molecular structure is an abiding theme of biochemical research.[2] The fabrication of specific 2D and 3D assemblies from small molecules by the process of self-assembly is a powerful strategy for the generation of functional materials and is also useful to unravel the mechanism of chemical basis of morphogenesis.[3] Design and synthesis of molecules with the ability to self-assemble to specific 3D shapes such as toroids and vesicles have attracted attention recently.[4] Despite the diverse applications of vesicles, the mechanism of their formation is not well understood.[5] Toroidal stuctures are observed in the self-assembly of proteins,[6] block copolymers,[4c-4d] surfactants[7] and other organic molecules.[4f-4g] Fabrication of toroidal nanostructures with uniform size and shape is a challenging endeavor, strategies such as flow-induced synthesis[8] and solidification of polymer droplets in a microfluidic device are used for this purpose.[9]

Here we present a class of triazolophanes with a hierarchical mechanism of assembly to toroids and vesicles. We envisaged that macrocyclic compounds incorporating aromatic and amide groups may impart rigidity and self-assemble to form a variety of 3D architectures based on conventional and non-coventional hydrogen bonds.[10] The triazole unit is considered as a mimic of an amide bond, apart from that it adds rigidity to the structure and provides a non-classical H-bond donor site.[11] We set out to synthesize a variety of triazolophanes making use of a Cu-catalyzed azide-alkyne cycloaddition (CuAAC) reaction. The first series of macrocycles based on an isophthaloyl unit resulted in insoluble compounds. The high insolubility of amide-linked isophthaloyl-based triazolophanes is believed to be as a result of intermolecular interactions due to its flat structure leading to strong π–π stacking and hydrogen bonding interactions. This prompted us to place a *t*-butyl substituent on the phenyl ring (Fig. 1) to reduce the intermolecular stacking interactions in order to improve the solubility. The cyclophanes **M1-M3** with amble rigidity and hydrogen bond donor and acceptor moieties are designed for investigating the self-assembly behavior.[12] Macrocycles **M1-M3** were synthesized by a CuAAC reaction between dialkynes and the corresponding diazides with ~40% yield (ESI†).

The relatively rigid molecular framework of **M1-M3** and the amide linkages confer them with self-assembling properties. The acidic triazole CHs are additional structural attributes of these molecules that can facilitate self-assembly by non-classical CH....X (X = O, N) interactions.

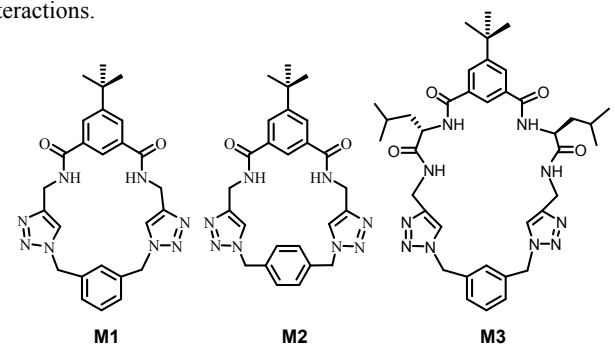

Figure 1: Structures of triazolophanes **M1**, **M2** and **M3**.

The self-assembly of **M1-M3** were studied by electron microscopy, atomic force microscopy (AFM) and X-ray crystal structure analysis. In order to probe the self-assembly of macrocycles, isomeric triazolophanes **M1** and **M2** with slight difference in the linker regions were synthesized. Macrocycle **M3** with leucine in the framework was synthesized in order to see the effect of chirality and macrocyclic size on the self-assembly.

Solutions of these compounds (**M1-M3)** with different concentrations in 1:1 chloroform:methanol were placed on freshly cleaned mica and allowed to evaporate in the air and analyzed by AFM. Mica provides a macroscale atomically flat surface by simply removing the top layers. This removes the influence of surface roughness on the self-assembly process. Careful analysis using AFM of a range of concentrations (0.1 mM to 1 mM) of triazolophanes revealed a variety of structures, such as hemi-toroids, toroids and vesicles. At 0.1 mM, the macrocycles show mostly hemi-toroids as

[a]*Department of Chemistry, Indian Institute of Technology Delhi (IITD), HauzKhas, New Delhi-110016, India. E-mail: haridasv@iitd.ac.in; h_haridas@hotmail.com; Tel: +91 01126591380*

[b]*Department of Chemistry, Keene State College, 229 Main Street, Keene, NH 03435-2001, USA. E-mail: jpjasinski@keene.edu*

†Electronic Supplementary Information (ESI) available: Details on synthesis, and data of all compounds. SEM, TEM, AFM images and crystallographic data. See DOI: 10.1039/c000000x/

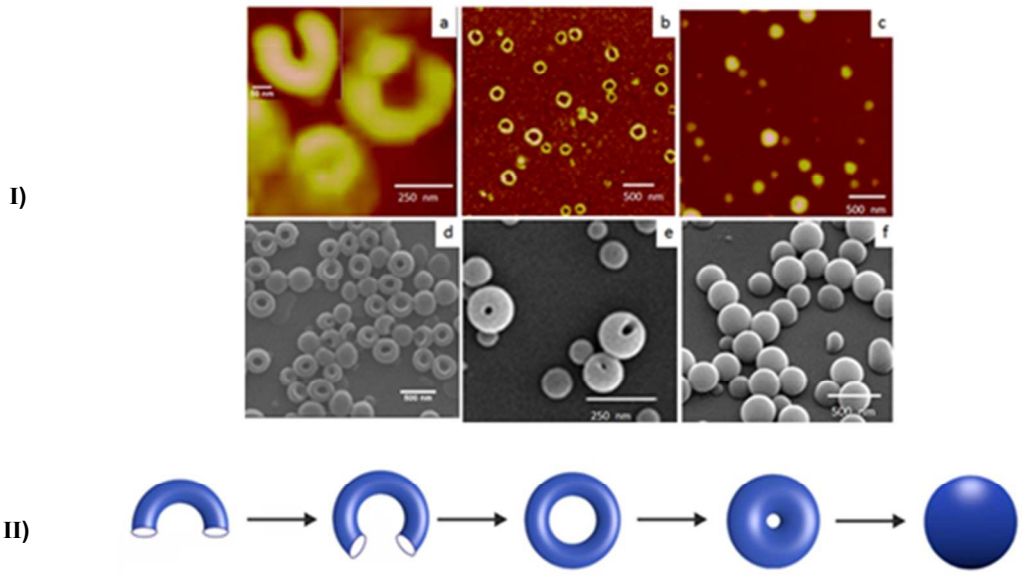

Figure 2: Ultramicroscopic analysis of the self-assembly of triazolophanes. Only selected images are presented **(I)** (a) AFM image of **M2** at 0.1 mM showing hemi-toroids. Inset shows a single magnified hemi-toroid (b) AFM image of **M2** at 0.25 mM showing the toroids (c) AFM image of **M2** at 1 mM showing the vesicles (d) SEM image of **M2** at 0.25 mM showing mostly toroids (e) FE-SEM image of **M2** at 0.5 mM showing toroids with decreasing internal cavity (f) FE-SEM and AFM image of **M2** at 1 mM showing vesicles **(II)** Schematic representation showing the evolution of vesicles. The increase in concentration results in transformation of hemi-toroids (left) to vesicles (right).

evident from AFM and transmission electron microscope (TEM) images (Fig. 2a and Fig. S1, ESI†). At about 0.25 mM concentration, mostly toroidal structures were observed (Figs. 2b, 2d, Figs. S1-S4, ESI†).

Scanning electron microscopic (SEM) analysis of **M2** showed diameters of toroids are in the range of 100-350 nm that match with the diameters of toroids of **M1** (Figs. S3 and S4, ESI†). Increasing the concentration resulted in the shrinkage of the internal cavity of the toroid (Figs. 2d-e). At 0.5 mM, toroids and vesicles were found to co-exist supporting the concentration effect on the self-assembly process. Analysis using AFM, TEM and SEM revealed the toroidal assembly at 0.25 mM (Fig. 2 and Figs. S1-S4, ESI†). The thickness and diameter of toroids are in the range of 45-80 nm and 100-450 nm respectively (Fig. 3). The AFM cross-sectional analysis further support the toroidal shape, albeit some flattening of the toroid due to adsorption to surface. The vertical height of the toroids is 20-30 nm and the horizontal diameter is 100-450 nm and the thickness 45-80 nm (Fig. 3). At 1 mM concentration, only vesicles were observed (Figs. 2c, 2f, and Figs. S1-S4), and vesicular evolution is schematically presented in Fig. 2.

Concentration dependent SEM and HR-TEM studies clearly show the same trend as also observed in AFM, and thus indicated that triazolophanes **M1**-**M3** form a hierarchical self-assembly pattern (Fig. 2, and Figs. S1-S7). The SEM analysis of **M1**-**M2** showed that the majority of the toroids and vesicles are in the range of 200-250 nm diameter (Figs. S3-S4, ESI†). The SEM and TEM data showed a good match on the dimensions of toroids and vesicles (Figs. S1, S3 and S4, ESI†). AFM also supported the same observation, but the dimension ranges are bit higher compared to SEM and TEM.[13]

The hemi-toroid is an intermediate structure formed en route to toroid, and toroid is in turn an intermediate self-assembled

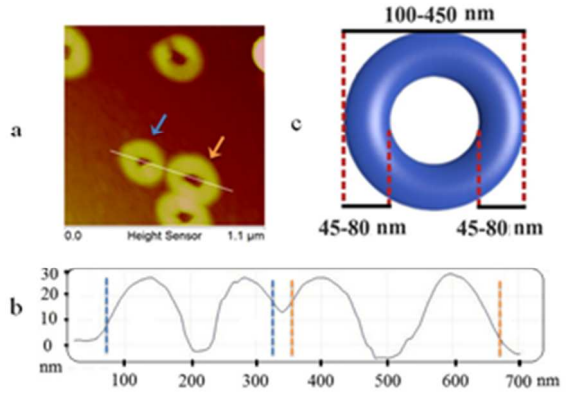

Figure 3: (a) AFM image of **M2** (b) Cross section along the line in (a). (c) Cartoon representation of toroid at 0.25 mM with dimensions estimated by SEM, TEM and AFM.

structure formed en route to becoming vesicles. Increasing concentration resulted in gradual changes from hemi-toroid to vesicles (Fig. 2). Similarly, dilution also resulted in vesicles to hemi-toroids, supporting that the transformations are bidirectional in nature. The definite concentration dependence on the topology indicates that the desired shape could be attained by change of concentration.

The macrocycle design can incorporate chiral units like amino acids in its framework. This has been demonstrated by synthesizing macrocycle **M3** containing leucine in its framework. Macrocycle **M3** shows self-assembly behavior similar to that of **M1**-**M2** (Fig. 2, and Figs. S5-S7, ESI†). This opens a wider opportunity for the design and synthesis of self-assembling amino acid-based triazolophanes. Interestingly, the CD spectrum of **M3** showed no characteristic CD signal indicating that the macrocycle has no specific folded conformation in solution. The

formation of vesicles for all macrocycles (**M1-M3**) follows the same path as revealed from their detailed ultra-microscopic studies (Fig. 2, Figs S1-S7, ESI†).

Dynamic light scattering (DLS) of **M2** and **M3** at different concentrations in 1:1 MeOH/$CHCl_3$, revealed the presence of particles with size in the range of ~198-478 nm, matching well with microscopic studies (Fig. S8, ESI†) demonstrating the presence of aggregate structures in solution.

SEM equipped with focused ion beam (FIB) was used to get finer details of toroids and vesicles (Fig. 4 and Fig. S9, ESI†).[14] The well-formed toroid from triazolophane **M2** was subjected to FIB milling using a gallium ion beam. The selected portion of the toroid was excised out (Figs. 4b, 4d) which revealed that the internal cavity of the toroid is empty.[15] Similarly, a portion of the vesicles from **M1** and **M3** were sliced off, which revealed the hollow interior (Fig. S9, ESI†).[16] Interestingly, in the TEM images, the thickness of membrane of the vesicles could not be seen, and hence appeared as dark spheres (Figs. S1c, S1f and S5c-5e, ESI†). This is also observed by other researchers and is attributed to the soft and rubbery-like nature of the vesicles.[17]

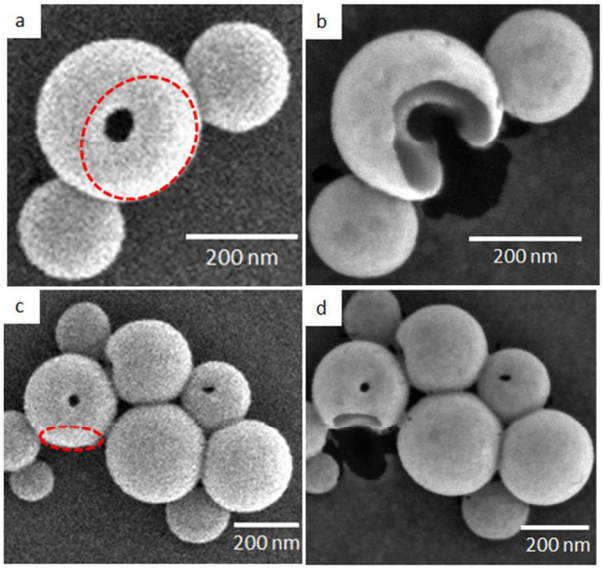

Figure 4: FE-SEM images of **M2** before (a and c) and after FIB milling (b and d). The red circles indicate the portions where FIB milling was performed. The observed surface softening of toroids after milling is due to high FIB energy employed in the experiment.[14]

To form closed 3D surfaces such as toroids and vesicles, a significant curvature in the self-assembly is required, suggesting a possible non-planar assembly adopted by triazolophane. In order to get insight into their self-assembly, we attempted crystallization of triazolophanes. Macrocycle **M2** was crystallized from a mixture of methanol, chloroform and acetonitrile. The X-ray crystal structure of macrocycle **M2** revealed an asymmetric unit comprised of two molecules of **M2** (Fig. 5a, Fig. S10 and Table S1, ESI†) which differ in the arrangement of triazole units. In one conformer, both the triazole CHs are pointing to same side (*syn*), while in the other, CHs of triazoles are pointing in opposite directions (*anti*). The amide carbonyls adopt an *anti*-conformation in both forms. The phenyl ring carrying *t*-butyl group is almost perpendicular to the plane of the 1,4-phenyl unit. The macrocycle **M2** has both a concave and convex surface. In the *syn* conformer, the nitrogens are on the concave face. The packing diagram reveals a very unique self-assembly pattern, in which different conformers of **M2** (*syn* and *anti*) arrange alternately to form a cyclic tetrad resembling a toroid (Fig. 5b, Figs. S11-S12, ESI†).[18]

Symmetry expansion reveals a circular tetrameric framework in the unit cell (maximum width 27 Å), in which each of the *syn* and *anti* molecules of **M2** are arranged in an alternate "up(*syn*)–down(*anti*)-down(*syn*)-up(*anti*)" fashion (Fig. S12, ESI†). The alternate "*syn–anti*" motif coupled with an up-down packing arrangement of the macrocycles results in the formation of a circular assembly with a hole positioned at the centre.

The tetrameric supramolecular assembly in the unit cell is held together by four CH….N and two CH….O hydrogen bonds (Table S2, ESI†). The methylene attached to the triazole of *anti* conformer bonds to the triazole nitrogen of the *syn* conformer (2.69Å), and one of the benzylic hydrogens of the *syn* conformer makes a non-covalent contact with the amide carbonyl of the *anti*-conformer (2.56Å). Each molecule in the tetrad makes three hydrogen bond contacts with its two neighbors (C25B-H25C····N6A**;** C15A-H15A····O2B and C25B-H25D····N3A). Both triazole moieties of the *syn* conformer take part in the hydrogen bonding. The *anti* conformer provides both the methylene protons attached to triazole and the amide carbonyl. A noteworthy point is that the molecules in the tetrad are held only by weak intermolecular non-classical hydrogen bonds. The tetrad assembly generates a hole at the centre that has a diameter of approximately ~10Å.

Careful analysis of the packing revealed that the *syn* conformers are assembled by two N-H…O (N1A-H1A····O2A**;** N8A-H8A····O1A) and two C-H…O interactions (C1A-H1AA····O1A**;** C23A-H23A····O1A) to form stacks

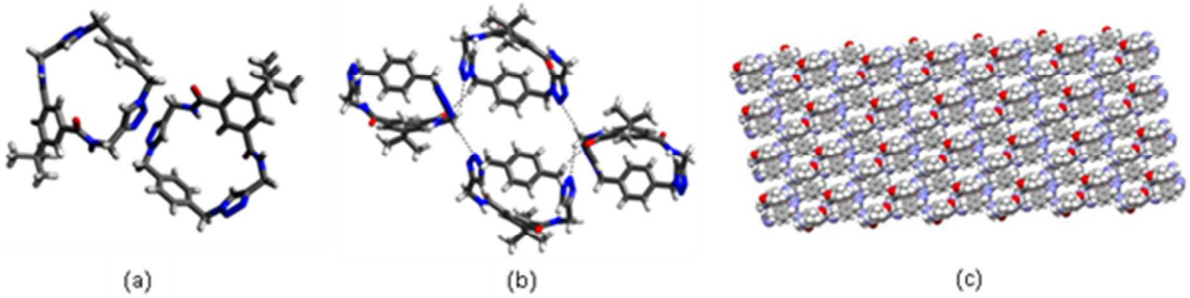

Figure 5: X-ray crystal structure of **M2**: (a) Capped stick representation of *syn* and *anti* conformers, (b) Capped stick representation showing tetrad assembly in the unit cell through hydrogen bonding, viewed along the b-axis (c) The packing diagram of **M2**, viewed along the b-axis. A small portion of the assembly is shown.

(Fig. S11, ESI†). In a similar way, *anti* conformers form stacks, wherein two intermolecular N-H…O (N1B-H1B···O2B**;** N8B-H8B···O1B) H-bonds are present. The separate *syn* and *anti* stacks indicate a clear case of self-sorting. The *syn* conformers in the tetrad make interactions with upper layer of *anti* conformers by (C15A-H15B···N6B**;** C15A-H15B···N7B) hydrogen bonds (Fig. S13, ESI†). Taken together the results from microscopic analysis and X-ray structure analysis imply that array of **M2,** with self-sorted stacks of *syn* and *anti* molecules and their inter stack interactions lead to a continuous surface (Fig. 5c), which may eventually fold into hemi-toroids, toroids and vesicles (Fig. S14, ESI†).

Bensimon and coworkers reported the self-assembly of phospholipids to various topological genuses.[19] Their experimental and theoretical studies indicated that the shape of vesicle is a result of minimization of its elastic curvature under various physical constraints. Our experimental results suggest that the intrinsic tendency of triazolophanes to form toroids may be due to its bent molecular architecture. The bent molecular shape causes spontaneous curvature to the assembly leading to minimum energy toroidal architecture. Increase in concentration leads to assembly of more molecules in the poloidal direction leading to vesicles (Fig. S14, ESI†).

In conclusion, we have designed, synthesized and studied the self-assembling behaviors of a series of triazolophanes by ultramicroscopy and X-ray crystallography. The studies presented here serve to support new hypothesis regarding the mechanism of vesicle formation. Furthermore, the 3D assemblies have many applications in chemistry and biology. The physio-chemical basis of vesicle morphogenesis from simple molecular building blocks has profound significance in evolutionary point of view. The concentration dependent self-assembly from hemi-toroid to vesicle through the intermediacy of a toroid is a new finding and we believe this study provide deep insight into the mechanism of vesicle formation. The finer details of the internal structure obtained from FIB milling experiments, support the hollow and robust nature of self-assembled structures.

We acknowledge DST, CSIR for financial support and IITD for instrumental facilities. We also acknowledge DST-FIST for HRMS and single crystal XRD facilities at IITD. We thank Prof. Narayanan Kurur and Prof. Nalin Pant, Department of Chemistry, IITD for discussions. We thank Prof. S. Aravindan and Mr. Amit Gupta, Department of Mechanical engineering, IITD for help in FIB experiments. JPJ acknowledges the NSF-MRI program (grant No. CHE-1039027) for funds to purchase the X-ray diffractometer.

Notes and references

1. (a) A. M. Turing, *Philos. Trans. R. Soc. B Biol. Sci.*, 1952, **237**, 37–72.
2. (a) S. I. Stupp, V. Lebonheur, K. Walker, L. S. Li, K. E. Huggins, M. Keser, A. Amstutz, *Science*, 1997, **276**, 384–389. (b) K. Petkau-Milroy and L. Brunsveld, *Org. Biomol. Chem.*, 2013, **11**, 219-232. (c) E. Gazit, *Chem. Soc. Rev.*, 2007, **36**, 1263-1269.
3. (a) J. M. Schnur, *Science*, 1993, **262**, 1669–1676. (b) N. B. Bowden, M. Weck, I. S. Choi and G. M. Whitesides, *Acc. Chem. Res.*, 2001, **34**, 231–238.
4. (a) M. C. M. van Oers, F. P. J. T. Rutjes and J. C. M. van Hest, *J. Am. Chem. Soc.*, 2013, **135**, 16308–16311. (b) Y. Kim, T. Kim and M. Lee, *Polym. Chem.*, 2013, **4**, 1300-1308. (c) Y. Kim, W. Li, S. Shin and M. Lee, *Acc. Chem. Res.*, 2013, **46**, 2888–2897. (d) L. Chen, T. Jiang, J. Lin and C. Cai, *Langmuir*, 2013, **29**, 8417–8426. (e) S. Yagai, S. Mahesh, Y. Kikkawa, K. Unoike, T. Karatsu, A. Kitamura and A. Ajayaghosh, *Angew. Chem. Int. Ed.*, 2008, **47**, 4691–4694. (f) S. Yagai, M. Yamauchi, A. Kobayashi, T. Karatsu, A. Kitamura, T. Ohba and Y. Kikkawa, *J. Am. Chem. Soc.*, 2012, **134**, 18205–18208. (g) Y. Lim and M. Lee, *J. Mater. Chem.*, 2011, **21**, 11680-11685. (h) K. Liu and L. Jiang, *ACS Nano*, 2011, **5**, 6786–6790. (i) Y. Wang and G. W. Padua, *Langmuir*, 2012, **28**, 2429–2435.
5. D. D. Lasic, *Biochem. J.*, 1988, **256**, 1-11.
6. M. M. Hingorani and M. O'Donnell, *Curr. Biol.*, 1998, **8**, R83–R86.
7. M. In, O. Aguerre-Chariol and R. Zana, *J. Phys. Chem. B*, 1999, **103**, 7747–7750.
8. J. J. Cardiel, L. Tonggu, A. C. Dohnalkova, P. de la Iglesia, D. C. Pozzo, L. Wang and A. Q. Shen, *ACS Nano*, 2013, **7**, 9704–9713.
9. B. Wang, H. C. Shum and D. A. Weitz, *ChemPhysChem*, 2009, **10**, 641–645.
10. (a) S. R. Seidel and P. J. Stang, *Acc. Chem. Res.*, 2002, **35**, 972–983. (b) W. Zhang and J. S. Moore, *Angew. Chem. Int. Ed.*, 2006, **45**, 4416–4439.
11. V. Haridas, S. Sahu, P. P. Praveen Kumar and A. R. Sapala, *RSC Adv.*, 2012, **2**, 12594-12605.
12. V. Haridas, S. Sahu and A. R. Sapala, *Chem. Commun.*, 2012, **48**, 3821-3823.
13. J. P. Patterson, M. P. Robin, C. Chassenieux, O. Colombani and R. K. O'Reilly, *Chem. Soc. Rev.*, 2014, **43**, 2412-2425.
14. R. J. Bailey, R. Geurts, D. J. Stokes, F. de Jong and A. H. Barber, *Micron*, 2013, **50**, 51–56.
15. J. Lee, K. Baek, M. Kim, G. Yun, Y. H. Ko, N.-S. Lee, I. Hwang, J. Kim, R. Natarajan, C. G. Park, W. Sung and K. Kim, *Nat. Chem.*, 2014, **6**, 97–103.
16. V. Haridas, M. B. Bijesh, A. Chandra, S. Sharma and A. Shandilya, *Chem. Commun*, 2014, **50**, 13797–13800.
17. M. Yang, W. Wang, F. Yuan, X. Zhang, J. Li, F. Liang, B. He, B. Minch and G. Wegner, *J. Am. Chem. Soc.*, 2005, **127**, 15107–15111.
18. R. M. McKinlay and J. L. Atwood, *Angew. Chem. Int. Ed.*, 2007, **46**, 2394–2397.
19. (a) X. Michalet and D. Bensimon, *Science*, 1995, **269**, 666–668. (b) B. Fourcade, M. Mutz and D. Bensimon, *Phys. Rev. Lett.*, 1992, **68**, 2551–2554.